

# **Modeling Mode Coupling Instability for Brake Noise**

- Introduction
- Literature Review
  - Common Brake Noises and their characterization
  - Theories about the underlying mechanisms
  - Minimal Models in literature
    - Stick-Slip Model (Shin et al.)
    - Mode Coupling Model (Hoffmann and Gaul)
  - Passive Control Strategies (Chatterjee)
- Mode Coupling Mechanism
  - Minimal Model: 2DOF Friction Oscillator
    - Mathematical Formulation
    - Stability Analysis
    - Mechanisms of Instability
    - Meaning of Stability in Time Domain
  - Setup of the Eigenvalue Problem
    - Base Model Parameters
  - Parameter Variation Studies
    - Stiffness Variation
    - Impact of Viscous Damping
  - Time-Domain Verification of Stability
  - Nonlinear and Time-Variant Analysis
    - Analysis of Geometric Nonlinearity
    - Analysis of Stiffness Variation
- Real Measurement Data
  - [REDACTED]
  - [REDACTED]
  - [REDACTED]
  - [REDACTED]
- Tuned Mass Damper (TMD)
  - Model Calibration
  - TMD System Setup
  - Parameter Study Design
  - TMD Parameter Study Results
  - Time-Domain Verification and Robustness Study

- Constant sinusoidal oscillation
  - Progressive Oscillation
  - Progressive-Regressive Oscillation
- Non-dimensional TMD
  - Nondimensionalization Procedure
    - Reference Scales
    - Stiffness Ratios
    - Damping Parameters
    - TMD Parameters
  - Nondimensional System Matrices
    - Mass Matrix
    - Damping Matrix
    - Stiffness Matrix (with coupling spring at angle  $\alpha = 45^\circ$ )
  - Key Dimensionless Groups
    - Friction-Coupling Parameter ( $\Pi_1$ )
    - Mode Frequency Ratio ( $\Pi_2$ )
  - Pi Groups Sweep Study and the Stability Boundary
    - Stability Map in  $\Pi_1$ - $\Pi_2$  Space
    - Nondimensional TMD Design Space
- Conclusion
- References

Authors: [@Yago Bas Fernandez](#) [@Matheus Ribeiro Vidal](#)

Supervisor: Markus Sailer

## Introduction

This project investigates the mode-coupling instability mechanism responsible for brake moan using a minimal model approach. The objectives are:

1. Understand the mechanism: Develop and analyze a 2DOF friction oscillator model that captures the essential physics of mode-coupling instability, including the role of friction-induced stiffness matrix asymmetry.
2. Validate against measurements: Calibrate the model to replicate a specific 260 Hz instability observed in experimental brake caliper data, establishing the connection between theoretical predictions and real-world behavior.

- Design a countermeasure: Extend the model to include a Tuned Mass Damper (TMD) and conduct parametric studies to identify robust design configurations that suppress the instability across varying operating conditions.

## Literature Review

A review of the state of the art in brake acoustics reveals that brake noise is traditionally characterized by its frequency range and the underlying triggering mechanism. This classification is essential for selecting the appropriate mathematical model for analysis.

### Common Brake Noises and their characterization

Brake noise phenomena are broadly categorized into low-frequency and high-frequency events:

Brake Noise Type	Frequency Range	Main Characteristics
<b>Judder</b>	<100 Hz	"Bremsmomentschwankung" (brake torque fluctuation)
<b>Groan &amp; Moan</b>	100 - 500 Hz	"dynamischen Instabilität des Systems Radbremse" (dynamic instability of the wheel brake system)
<b>Howl</b>	500 - 1000 Hz	Higher frequency range dynamic instability of the wheel brake system
<b>LF Squeal</b>	1 - 3 kHz	"selbsterregte Schwingung der Radbremse" (self-excited vibration of the wheel brake)
<b>HF Squeal</b>	3 - 20 kHz	

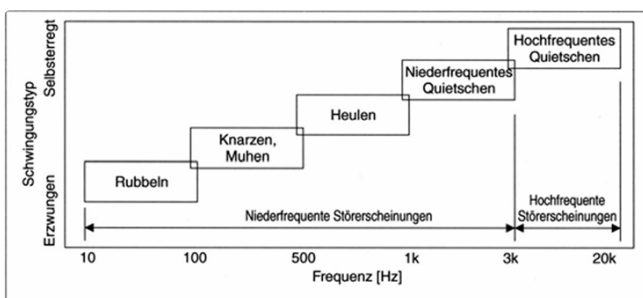


**Bild 22-1** Einteilung der Schwingungen und Geräusche beim Bremsen nach [8]

B. Breuer & K. H. Bill (2003)

## Theories about the underlying mechanisms

The literature identifies three primary mechanisms responsible for self-excitation in brake systems:

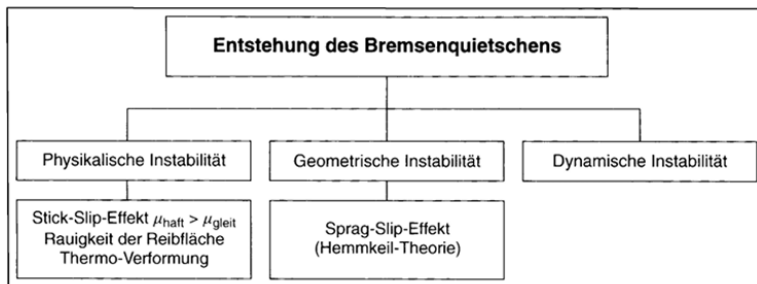


**Bild 22-4** Mechanismen der Quietschentstehung nach [5]

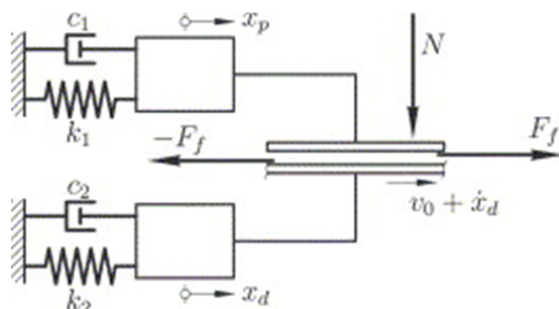
B. Breuer & K. H. Bill (2003)

- **Physical Instability (Stick-Slip):** Driven by a difference between static and kinetic friction coefficients ( $\mu_s > \mu_k$ ) or a negative friction-velocity slope. This is the root cause of creep groan.
- **Geometric Instability (Sprag-Slip):** Also known as the jamming wedge effect, where kinematic constraints induce locking.
- **Dynamic Instability (Mode Coupling):** This is the primary cause of high-frequency squeal. It occurs when component resonances couple due to the non-conservative friction forces, leading to instability even with a constant friction coefficient.

## Minimal Models in literature

To analyze these mechanisms, "Minimal Models" (simplified lumped-parameter systems) are widely used to reduce computational complexity while capturing the fundamental physics. Two known models were reviewed:

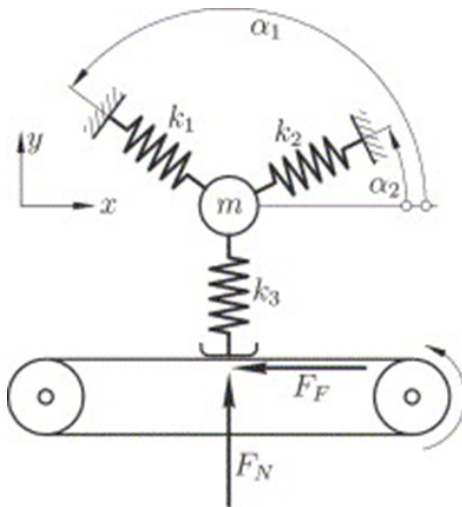
### Stick-Slip Model (Shin et al.)



Shin et al. (2002)

The model proposed by Shin et al. utilizes a 2-degree-of-freedom (2DOF) system to investigate stick-slip phenomena. This model focuses on the alternating "stick" (adhesion) and "slip" phases at the friction interface. While effective for analyzing creep groan and low-speed vibrations triggered by falling friction characteristics ( $\mu_s > \mu_k$ ), it does not primarily address the geometric mode coupling responsible for high-frequency squeal.

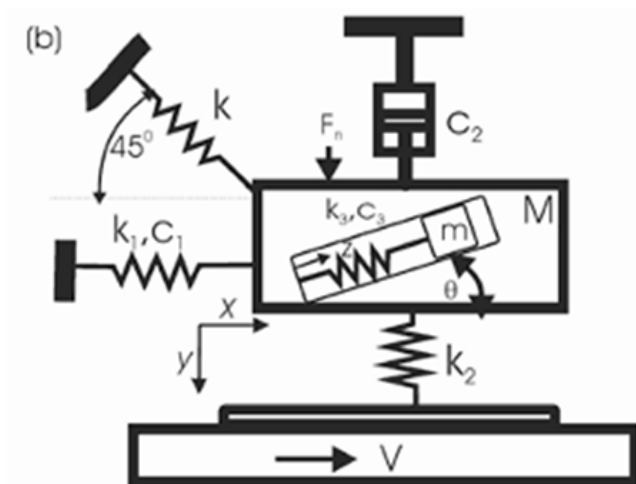
## Mode Coupling Model (Hoffmann and Gaul)



Hoffmann et al. (2002)

This 2DOF model demonstrates that instability can arise purely from the geometry of the system. In this formulation, displacements normal to the friction surface are coupled with tangential motions. The friction force acts as a non-conservative "cross-coupling" force, transferring energy from the sliding contact into vibrational energy. This mechanism aligns with the "Binary Flutter" or "Coalescence" theory, where two stable eigenmodes merge to form an unstable complex conjugate pair, making it the preferred approach for modeling the 260 Hz instability observed in this project.

## Passive Control Strategies (Chatterjee)



Chatterjee (2006)

While the previously mentioned models focus on the mechanisms generating instability, Chatterjee [5] extended the analysis to investigate the suppression of these vibrations. The study utilized a minimal model incorporating both mode coupling and velocity-weakening friction to evaluate the efficacy of a Dynamic Vibration Absorber (DVA). The research established critical design criteria for the absorber, demonstrating that robust stability is

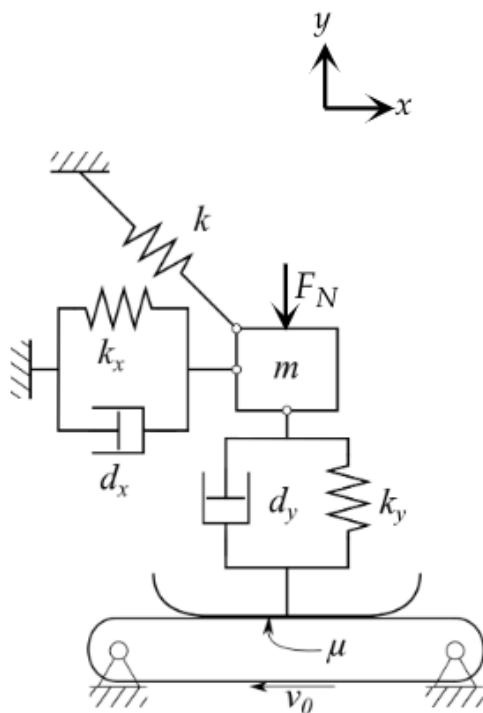
achieved by optimizing the absorber's damping and tuning ratio to maximize the decay rate (negative real part) of the unstable eigenvalues. This work provides the theoretical foundation for using a Tuned Mass Damper (TMD) as a countermeasure for friction-induced instability.

## Mode Coupling Mechanism

To understand the phenomenon of brake squeal, it is essential to analyze the mechanism of mode coupling instability. This section introduces a minimal mechanical model that demonstrates how friction-induced self-excited vibrations arise from the coupling of structural modes.

### Minimal Model: 2DOF Friction Oscillator

The mechanism is illustrated using a minimal model consisting of a 2-degree-of-freedom (2DOF) friction oscillator, as originally proposed by Schroth (2003). The system comprises a mass connected to a fixed structure via springs and dampers in orthogonal directions ( $x$  and  $y$ ).



Source: Schroth 2003

Schematic of the 2DOF Friction Oscillator (Source: Schroth, 2003)

A mass is supported by springs and dampers in  $x$  and  $y$  directions, with an angular coupling spring  $k$ . It slides on a belt moving at velocity  $v_0$ .

The key components of the model are:

- **Stiffness and Damping:** The system includes stiffnesses  $\sigma \leq 0$  and  $k_y$ , along with dampers  $d_x$  and  $d_y$ .
- **Coupling Element:** A coupling spring  $k$  connects the mass at an angle, which is necessary to induce mode coupling between the  $x$  and  $y$  degrees of freedom.
- **Friction Interface:** The mass is tied to a sled sliding on a moving belt with a velocity  $v_0$ . A crucial assumption in this model is that the sliding friction coefficient  $\mu$  is constant and independent of the belt velocity ( $\mu = \text{const}$ ). This distinguishes mode coupling from other instability mechanisms that rely on a velocity-dependent friction coefficient.

## Mathematical Formulation

The dynamics of the system are governed by the equation of motion in matrix form:

$$\mathbf{M}\ddot{\mathbf{x}} + \mathbf{D}\dot{\mathbf{x}} + \mathbf{K}\mathbf{x} = \mathbf{f}$$

where  $M$ ,  $D$ , and  $K$  represent the mass, damping, and stiffness matrices, respectively.

The displacement vector is defined as  $\mathbf{x} = [x, y]^T$ .

The friction force is proportional to the normal force ( $F_R = \mu F_N$ ). In this formulation, the friction term introduces off-diagonal elements into the stiffness matrix. Unlike standard structural systems, this friction term renders the stiffness matrix *unsymmetric*:

$$\mathbf{K} = \begin{bmatrix} k_x + \frac{1}{2}k & -\frac{1}{2}k + \mu(k_y + \frac{1}{2}k) \\ -\frac{1}{2}k & k_y + \frac{1}{2}k \end{bmatrix}$$

To analyze the stability, the second-order ordinary differential equation is reduced to a first-order state-space equation:

$$\dot{\mathbf{x}}(t) = \mathbf{A}\mathbf{x}(t) + \mathbf{b}$$

Here, the state vector is expanded to include velocities:  $\mathbf{z} = [x, y, \dot{x}, \dot{y}]^T$ . The system matrix  $A$  is derived as follows:

$$A = \begin{bmatrix} \mathbf{0} & I \\ -M^{-1}\widehat{K} & -M^{-1}D \end{bmatrix}$$

The vector  $b$  accounts for the stationary forces. The stationary point of the system is defined where  $\dot{\mathbf{x}}(t) = \mathbf{0}$ .

## Stability Analysis

The stability of the system is determined by the eigenvalues  $\lambda$  of the system matrix  $A$ . These are calculated by solving the characteristic polynomial:

$$p(\lambda) = \det(A - \lambda I) = \frac{1}{\det M} \det(M\lambda^2 + D\lambda + \widehat{K}) = 0$$

The solution yields complex eigenvalues in the form:

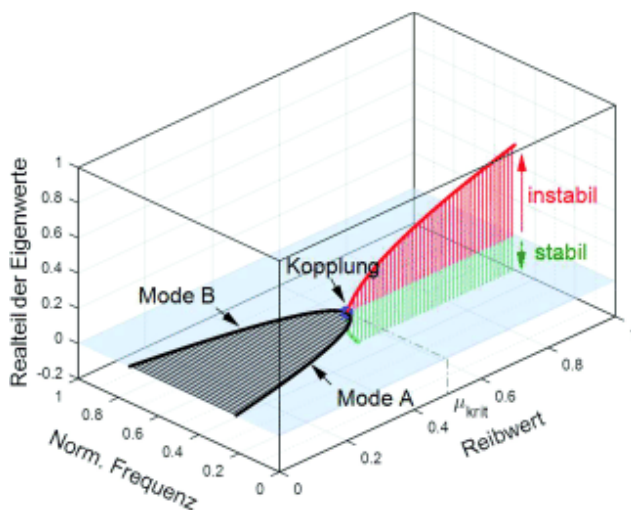
$$\lambda = \sigma \pm i\omega$$

where  $\sigma$  is the real part (decay/growth rate) and  $\omega$  is the imaginary part (frequency). The stability criterion is based strictly on the real part  $\sigma$ :

- **Stable ( $\sigma < 0$ ):** The mode is damped, and perturbations decline over time.
- **Limit Stable ( $\sigma = 0$ ):** The system is at the stability boundary.
- **Unstable ( $\sigma > 0$ ):** The system exhibits exponential growth, physically interpreted as “negative damping”.

## Mechanisms of Instability

Mode coupling instability is triggered when the friction coefficient  $\mu$  exceeds a critical value, denoted as  $\mu_{\text{crit}}$ .



Evolution of eigenvalues with increasing friction (Source: Marschner, 2017).

As  $\mu$  increases, frequencies coalesce. Beyond  $\mu_{\text{crit}}$ , the real part of one mode becomes positive, indicating instability.

The process occurs in two stages:

- **Frequency Coalescence:** As  $\mu$  increases, the eigenfrequencies of two distinct structural modes approach each other. At  $\mu = \mu_{\text{crit}}$ , these frequencies merge.

- **Bifurcation:** Beyond this critical friction value ( $\mu > \mu_{\text{crit}}$ ), the eigenvalues split. One conjugate pair develops a positive real part ( $\sigma > 0$ ), while the other becomes more heavily damped.

This mathematical bifurcation corresponds to the physical phenomenon where the unsymmetric stiffness matrix couples the modes, pumping energy into the system and generating the self-excited vibrations characteristic of brake noise.

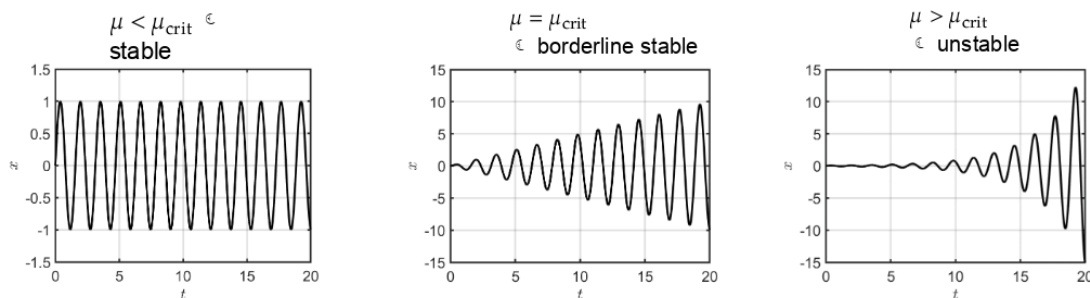
## Meaning of Stability in Time Domain

The physical interpretation of the stability criterion can be visualized by examining the system's time-domain response. The solution to the initial value problem is assumed to take the form of an exponential Ansatz:

$$\mathbf{z}(t) = \hat{\mathbf{z}}e^{\lambda t} = \hat{\mathbf{z}}e^{(\sigma+i\omega)t} = \hat{\mathbf{z}}e^{\sigma t}(\cos(\omega t) + i \sin(\omega t))$$

where  $\lambda = \sigma + i\omega$  is the complex eigenvalue. The stability is governed entirely by the real part  $\sigma$ :

- The term  $e^{i\omega t}$  represents the oscillatory component (harmonic vibration).
- The term  $e^{\sigma t}$  represents the amplitude envelope (growth or decay).



Time-domain interpretation of stability

As illustrated in the stability diagram, the system behavior changes distinctively with the friction coefficient  $\mu$ :

- **Stable Regime ( $\mu < \mu_{\text{crit}}$ ):** The real part  $\sigma$  is zero (or negative in damped systems). The system exhibits stable harmonic oscillations where the amplitude remains constant or decays over time.
- **Borderline Stability ( $\mu = \mu_{\text{crit}}$ ):** This represents the bifurcation point where the system transitions from stable to unstable behavior.
- **Unstable Regime ( $\mu > \mu_{\text{crit}}$ ):** The real part  $\sigma$  becomes positive ( $\sigma > 0$ ). The term  $e^{\sigma t}$  causes the oscillation amplitude to grow exponentially, which physically manifests as brake noise.

## Setup of the Eigenvalue Problem

### Base Model Parameters

m [kg]	$\mu$	$k_x$ [N/m]	$k_y$ [N/m]	$k$ [N/m]	$d_x$ [N·s·m <sup>-1</sup> ]	$d_y$ [N·s·m <sup>-1</sup> ]
1	[0-0.6]	11	20	10	0	0

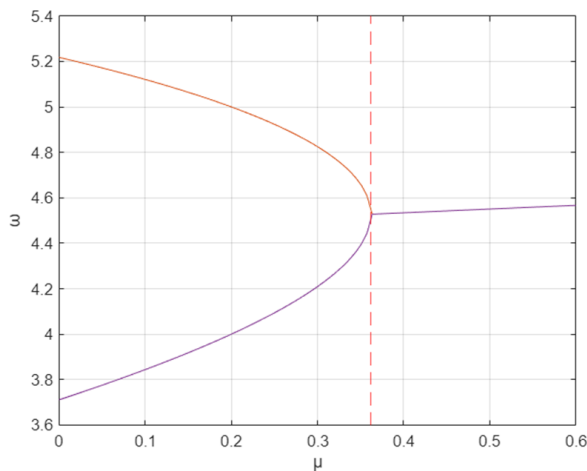
The baseline analysis assumes an undamped system. The equation of motion in matrix form shows as follows:

$$\begin{bmatrix} m & 0 \\ 0 & m \end{bmatrix} \begin{Bmatrix} \ddot{x} \\ \ddot{y} \end{Bmatrix} + \begin{bmatrix} d_x & 0 \\ 0 & d_y \end{bmatrix} \begin{Bmatrix} \dot{x} \\ \dot{y} \end{Bmatrix} + \begin{bmatrix} k_x + \frac{1}{2}k & -\frac{1}{2}k + \mu(k_y + \frac{1}{2}k) \\ -\frac{1}{2}k & k_y + \frac{1}{2}k \end{bmatrix} \begin{Bmatrix} x \\ y \end{Bmatrix} = \begin{Bmatrix} -\mu \\ -1 \end{Bmatrix} F_N$$

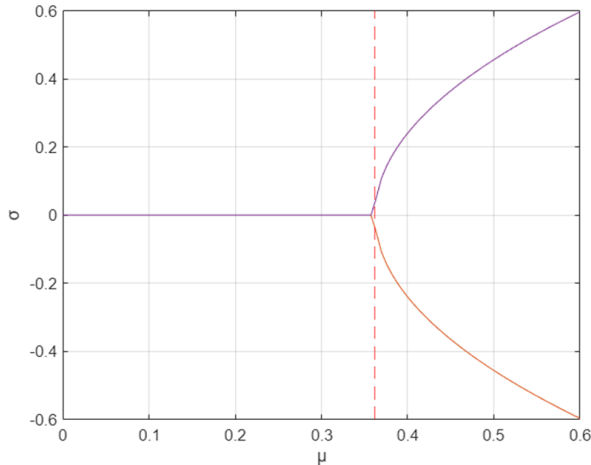
The stability analysis is performed by numerically solving for the roots of the characteristic polynomial derived from the state-space matrix  $A$ . The simulation defines a friction coefficient vector  $\mu$  ranging from 0 to 0.6, discretized into 100 steps. For each step, the complex eigenvalues  $\lambda = \sigma \pm i\omega$  are computed.

The critical friction coefficient  $\mu_{\text{crit}}$ , which marks the onset of instability, is calculated analytically using the discriminant of the characteristic polynomial. For the given example:

$$\mu_{\text{crit}} = 0.3620$$



Imaginary part of the eigenvalues with respect to friction coefficient



Real part of the eigenvalues with respect to friction coefficient

The already mentioned frequency coalescence and bifurcation appear clearly in the performed stability analysis. When the friction coefficient reaches its critical value, the frequencies couple together and the growth rate develops positive values as consequence of the mode coupling phenomena.

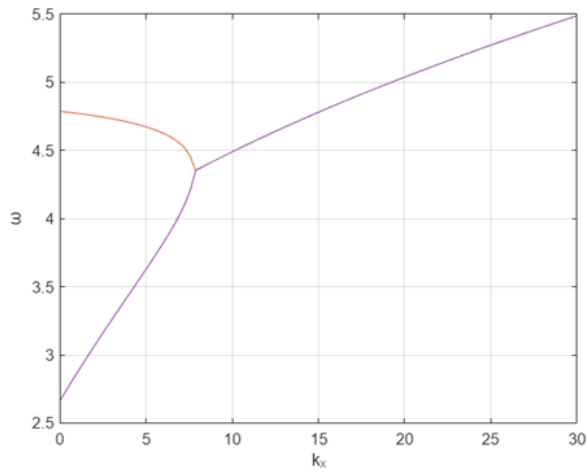
## Parameter Variation Studies

Three specific parameter studies were conducted to assess design sensitivities:

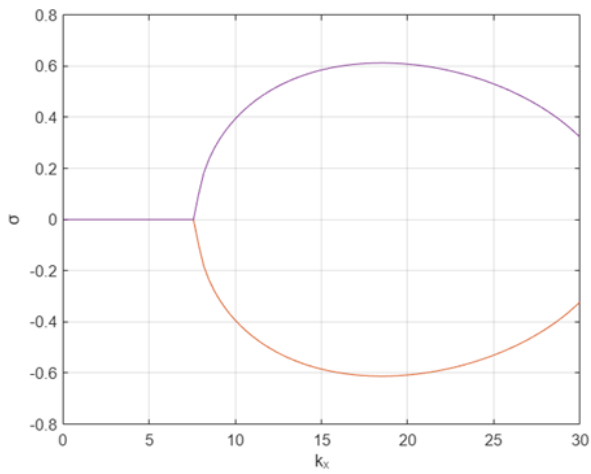
### Stiffness Variation

To understand the influence of structural stiffness on mode coupling, the stiffness parameters ( $k_x$ ,  $k_y$ , and the coupling stiffness  $k_c$ ) were varied independently within a range of  $[0, 30]$ .

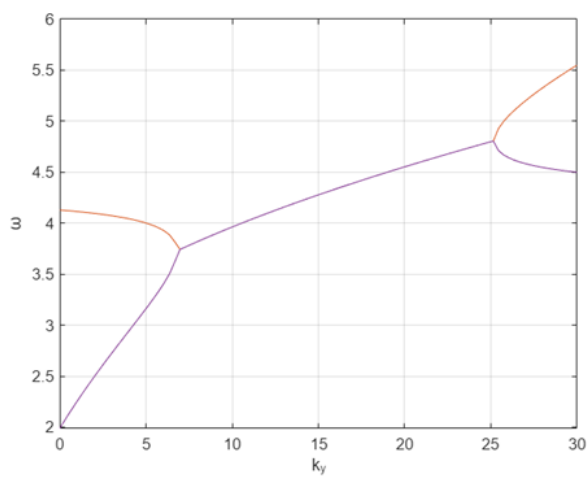
- The friction coefficient was fixed at an unstable value of  $\mu = 0.5$ .
- Each stiffness parameter was varied while holding the others constant at their base values.
- The goal is to identify stiffness regions that suppress the instability (i.e., yield  $\sigma \leq 0$ ) despite the high friction level.



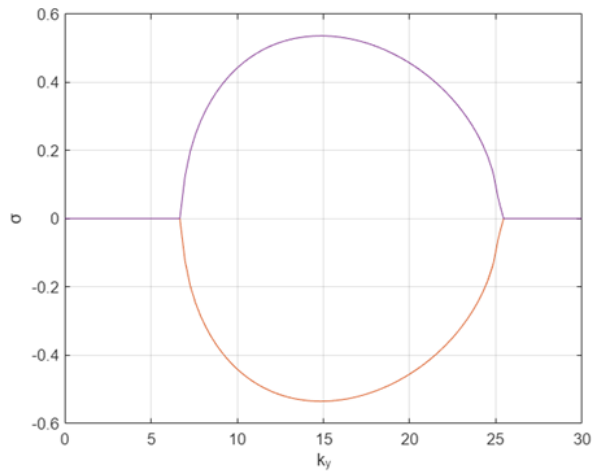
Imaginary part over stiffness  $k_x$



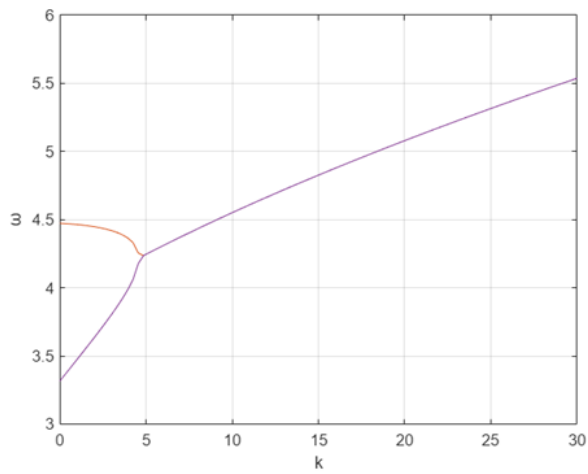
Real part over stiffness  $k_x$



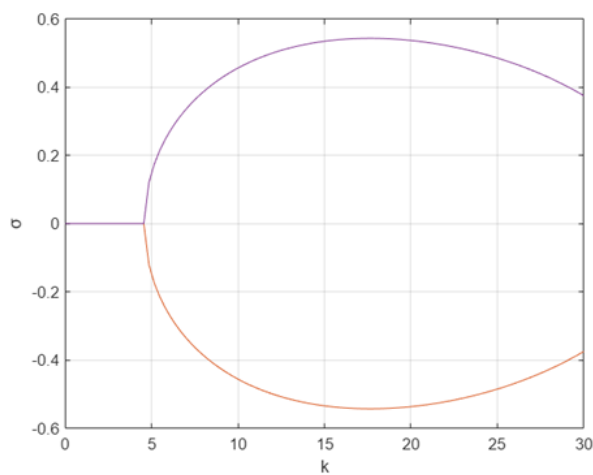
Imaginary part over stiffness  $k_y$



Real part over stiffness  $k_y$



Imaginary part over stiffness  $k$



Real part over stiffness  $k$

From the plots above it can be inferred that:

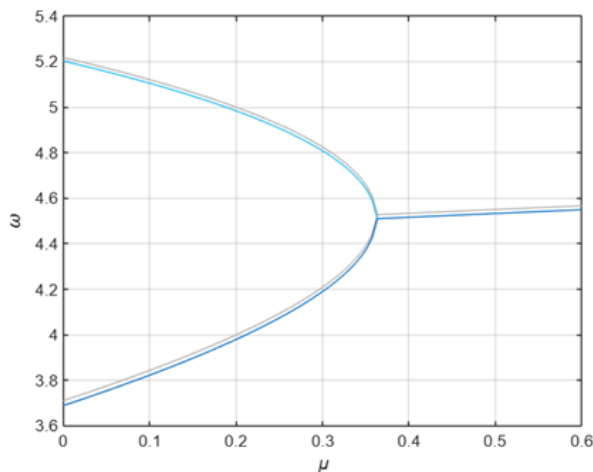
- increasing the coupling stiffness  $k$  or the horizontal stiffness  $k_x$  tends to drive the system into this coalesced, unstable state.
- The vertical stiffness  $k_y$  demonstrates that stability can be restored by “detuning” the system; sufficiently increasing or decreasing  $k_y$  separates the eigenfrequencies, preventing coalescence and suppressing the instability.

This confirms that modifying structural stiffness to separate modal frequencies is an effective design strategy to avoid mode coupling instability.

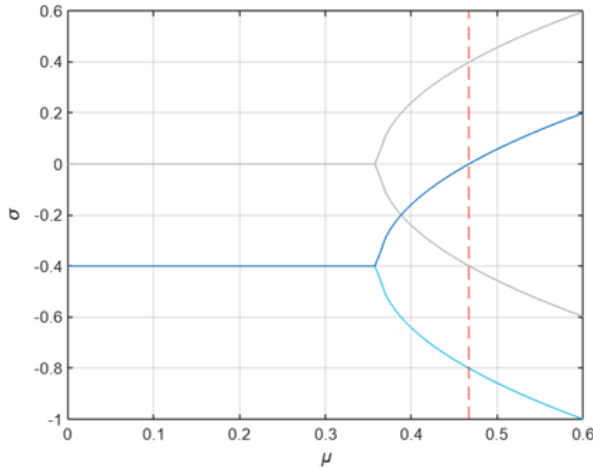
### Impact of Viscous Damping

This study introduces viscous damping to the system to evaluate its stabilizing effect. Two damping scenarios are simulated and in both damping cases, the friction coefficient  $\mu$  is swept from 0 to 0.6 to determine the new critical friction value  $\mu_{crit}$  relative to the undamped case.

- **Symmetric Damping:** Equal damping is applied to both degrees of freedom ( $d_x = d_y = 0.7$ ).



Imaginary part over friction. (Undamped = Gray, Damped = Blue)

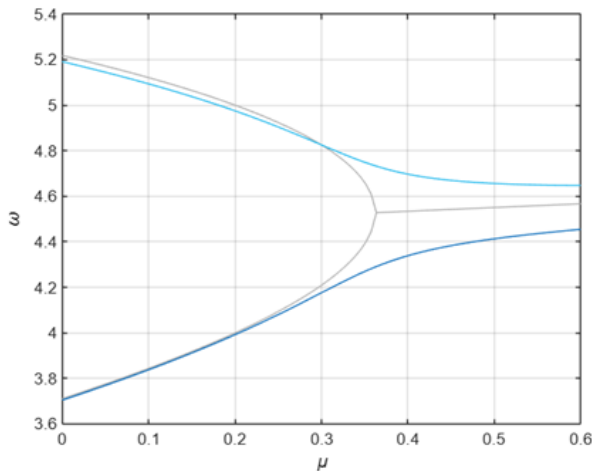


Real part over friction. (Undamped = Gray, Damped = Blue)

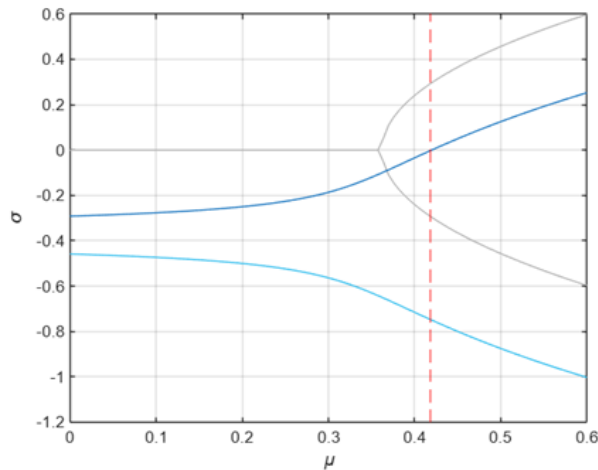
The symmetric damping initializes the system with a negative real part ( $\sigma < 0$ ). This reflects the energy dissipation introduced by the dampers. Although the splitting of the eigenvalues occurs at approximately the same friction value as the undamped case ( $\mu \approx 0.36$ ), the system remains stable for a wider range. Because the real part curve is shifted downwards, the upper branch of the eigenvalue pair requires a higher friction coefficient to cross the zero axis. Consequently, the critical friction value increases from  $\mu_{crit} = 0.3620$  to  $\mu_{crit} \approx 0.4$ .

This confirms that symmetric damping effectively delays the onset of brake squeal.

- **Asymmetric Damping:** Unequal damping is applied ( $d_y = 1, d_x = 0.5$ ) to observe how damping distribution affects the critical friction value.



Imaginary part over friction. (Undamped = Gray, Damped = Blue)



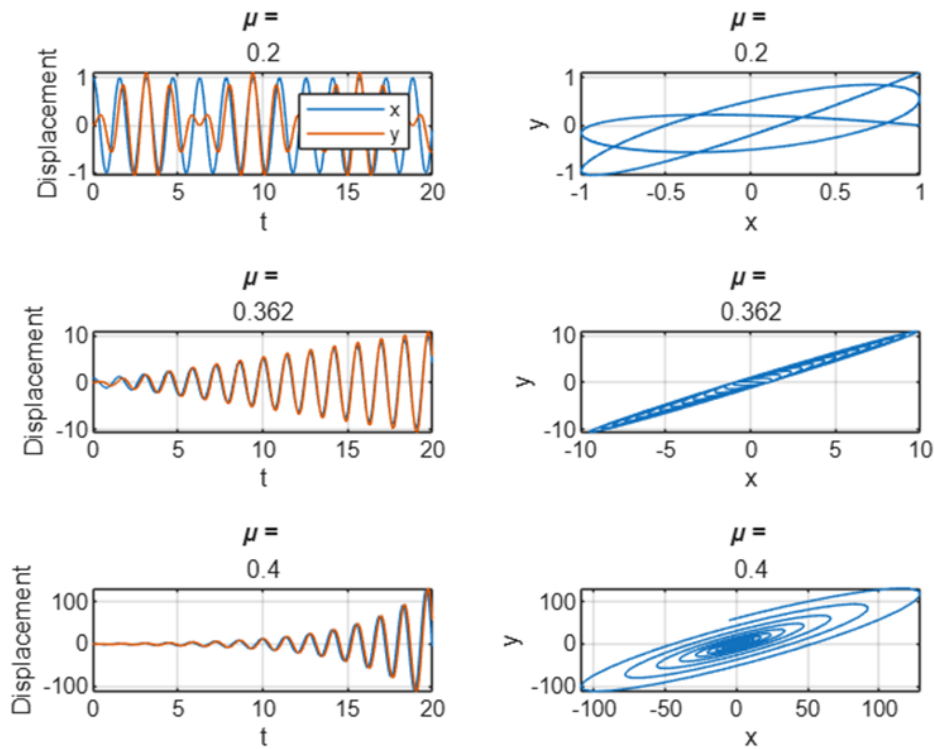
Real part over friction. (Undamped = Gray, Damped = Blue)

In the second scenario, the frequencies approach each other but show a “smoothing” effect rather than a sharp coupling. Similar to the symmetric case, the real parts begin in the negative region. The instability is again delayed compared to the undamped case.

The study concludes that adding viscous damping is a robust strategy for suppressing mode coupling instability. By dissipating energy, damping requires the friction forces to pump significantly more energy into the system before self-excited vibrations can grow, effectively shifting the stability boundary to higher, safer friction levels.

### Time-Domain Verification of Stability

To validate the eigenvalue analysis performed in the previous sections, the system’s response was simulated in the time domain using numerical integration of the state equations. The simulation compares the displacement  $x(t)$  and the phase space trajectory ( $y$  vs  $x$ ) for three distinct friction regimes: stable, critical, and unstable.

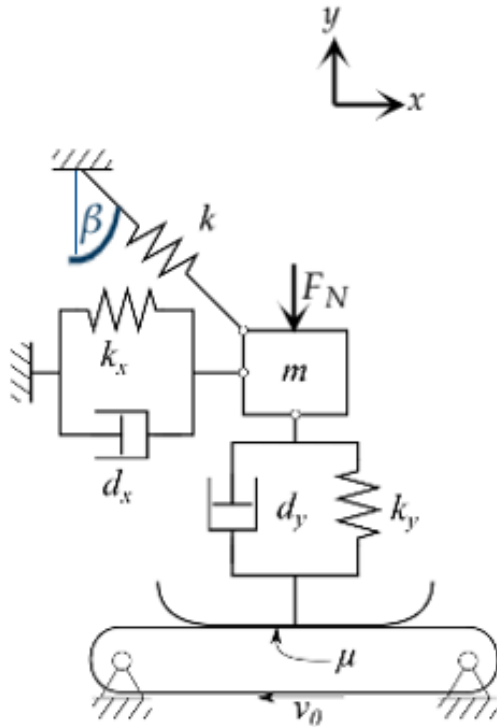


Time-domain response (left) and phase portraits (right) for stable ( $\mu = 0.2$ ), critical ( $\mu = 0.362$ ), and unstable ( $\mu = 0.4$ ) friction coefficients.

- **Stable Regime ( $\mu < \mu_{crit}$ ):** displacement exhibits bounded oscillations with no significant growth, meaning the amplitude remains constant or decays slowly (depending on numerical damping), confirming that the real part of the eigenvalues is non-positive ( $\sigma \leq 0$ ). In the phase plot, while the  $x$  and  $y$  degrees of freedom are coupled, they oscillate with a distinct phase difference and potentially distinct frequencies.
- **Borderline Stability ( $\mu = \mu_{crit}$ ):** The time-domain plot shows the beginning of amplitude growth, marking the transition from stability to instability. The phase portrait turns into a narrow diagonal loop. This geometric change is the physical manifestation of *frequency coalescence*. As the imaginary parts of the eigenvalues merge, the  $x$  and  $y$  modes synchronize perfectly. They become "locked" in phase, vibrating along a unified vector rather than orbiting independently.
- **Unstable Regime ( $\mu > \mu_{crit}$ ):** The time-domain response shows explosive exponential growth within a short interval. This confirms that the real part of the eigenvalue has split and become positive. The phase portrait expands rapidly as a straight diagonal spiral. The linearity of this trajectory confirms that the frequencies remain merged.

## Nonlinear and Time-Variant Analysis

This section extends the analysis to the time domain to investigate two specific nonlinear effects: geometric nonlinearity in the coupling angle  $\beta$  and time-harmonic variation of the vertical stiffness  $k_y$ .



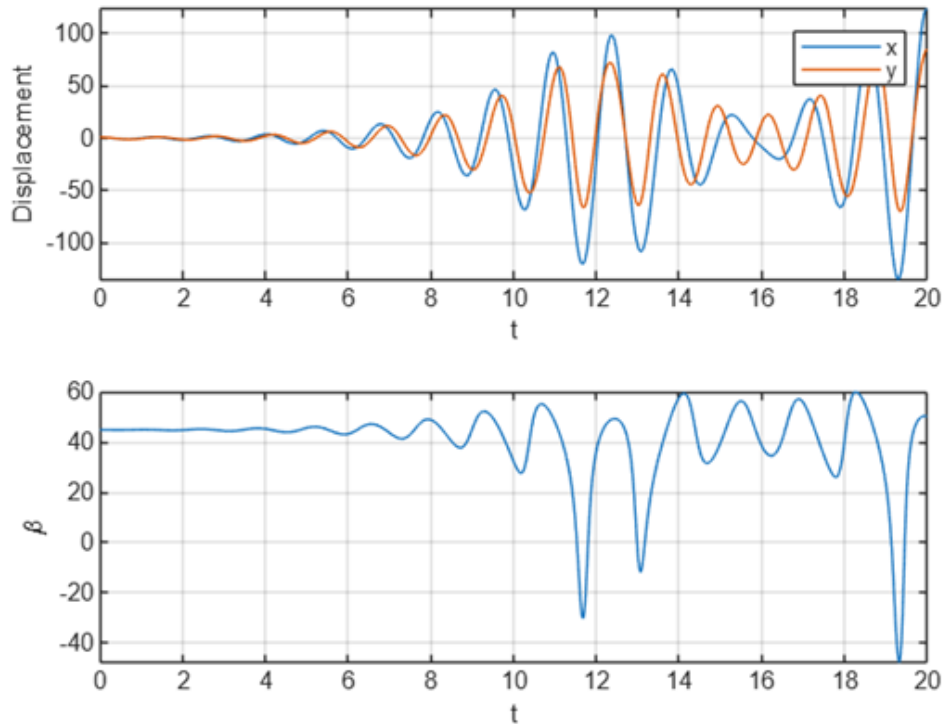
Schematic of the non-linear 2DOF Friction Oscillator

In the linear model, the coupling spring angle was fixed ( $45^\circ$ ). In this analysis, the angle  $\beta$  is allowed to vary dynamically as a function of the mass displacement. The angle  $\beta(t)$  is calculated at each time step based on the instantaneous position of the mass  $(x, y)$  relative to the spring's anchor point. Consequently, the stiffness matrix  $\mathbf{K}$  becomes state-dependent ( $\mathbf{K}(x)$ ). The terms previously defined by fixed constants are replaced by their trigonometric counterparts:

$$\mathbf{K}(\beta) = \begin{bmatrix} k_x + k \sin^2(\beta) & -k \sin(\beta) \cos(\beta) + \mu(k_y + k \sin(\beta) \cos(\beta)) \\ -k \sin(\beta) \cos(\beta) & k_y + k \cos^2(\beta) \end{bmatrix}$$

The system is simulated with an initial displacement perturbation to observe if the small variations in  $\beta$  introduce instability in a nominally stable friction regime. The friction coefficient for this case is  $\mu = 0.5$ ; e.g., in the unstable regime.

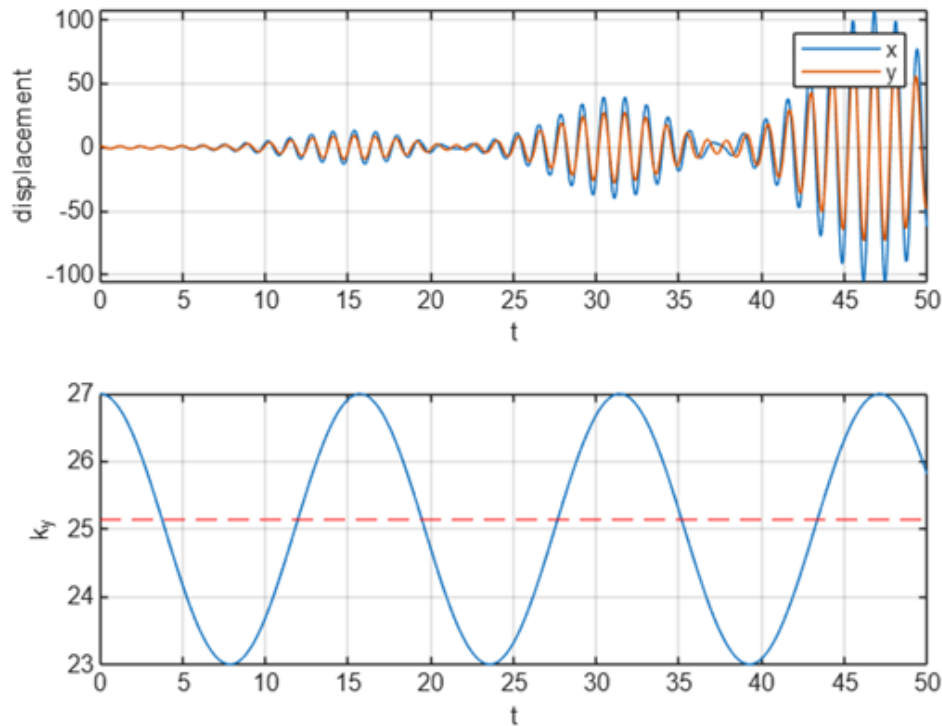
## Analysis of Geometric Nonlinearity



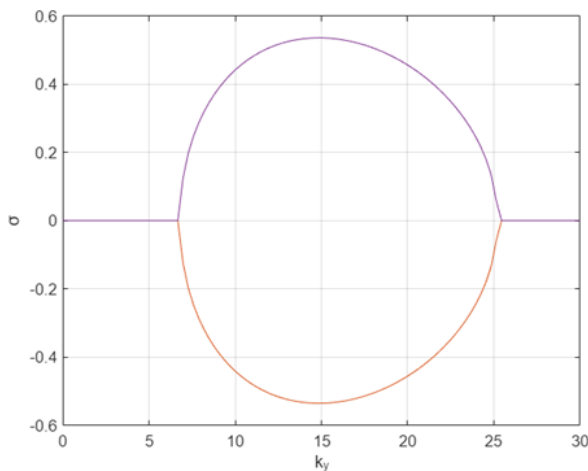
System response with variable coupling angle  $\beta(t)$  at  $\mu = 0.5$ . Top: Divergent displacement in  $x$  and  $y$ . Bottom: Large fluctuations of the angle  $\beta$  driven by the growing amplitude.

The simulation results confirm that the geometric nonlinearity does not suppress the instability at the selected friction level ( $\mu = 0.5$ ). As the vibration amplitude increases, the coupling angle  $\beta$  (bottom plot) deviates significantly from its nominal value of  $45^\circ$ , oscillating wildly between  $-40^\circ$  and  $+60^\circ$ . While the changing angle continuously modifies the stiffness matrix  $K(\beta)$ , it does not act as a saturation mechanism in this time window.

## Analysis of Stiffness Variation



System response under parametric stiffness variation. Top: Displacement  $x(t)$  and  $y(t)$ . Bottom: Time-variant stiffness  $k_y(t)$



Stability threshold derived from the previous parameter study: Real part over stiffness  $k_y$  with  $\mu = 0.5$

- When  $k_y < 25.15$ , the system enters the unstable mode coupling region.
- When  $k_y > 25.15$ , the system enters the stable region where eigenfrequencies are detuned.

The vibration amplitude grows rapidly during the unstable intervals and stabilizes (stops growing exponentially) during the stable intervals. Despite the existence of stable intervals, the overall trend is divergent. The energy pumped into the system during the unstable phases

exceeds any dissipation or stabilization during the stable phases, confirming that periodic parameter fluctuations crossing the stability boundary are sufficient to sustain and amplify brake noise.

### Real Measurement Data

[Redacted]

[Redacted]

[Redacted]

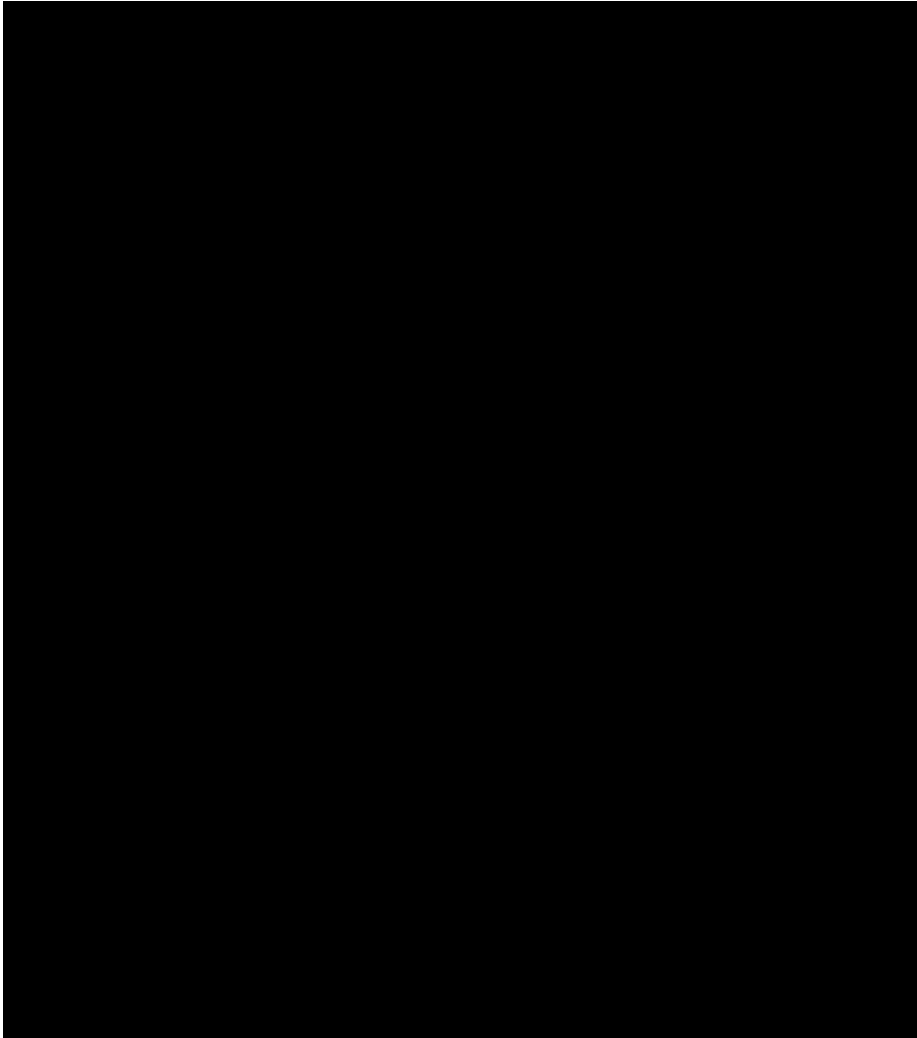
[Redacted]

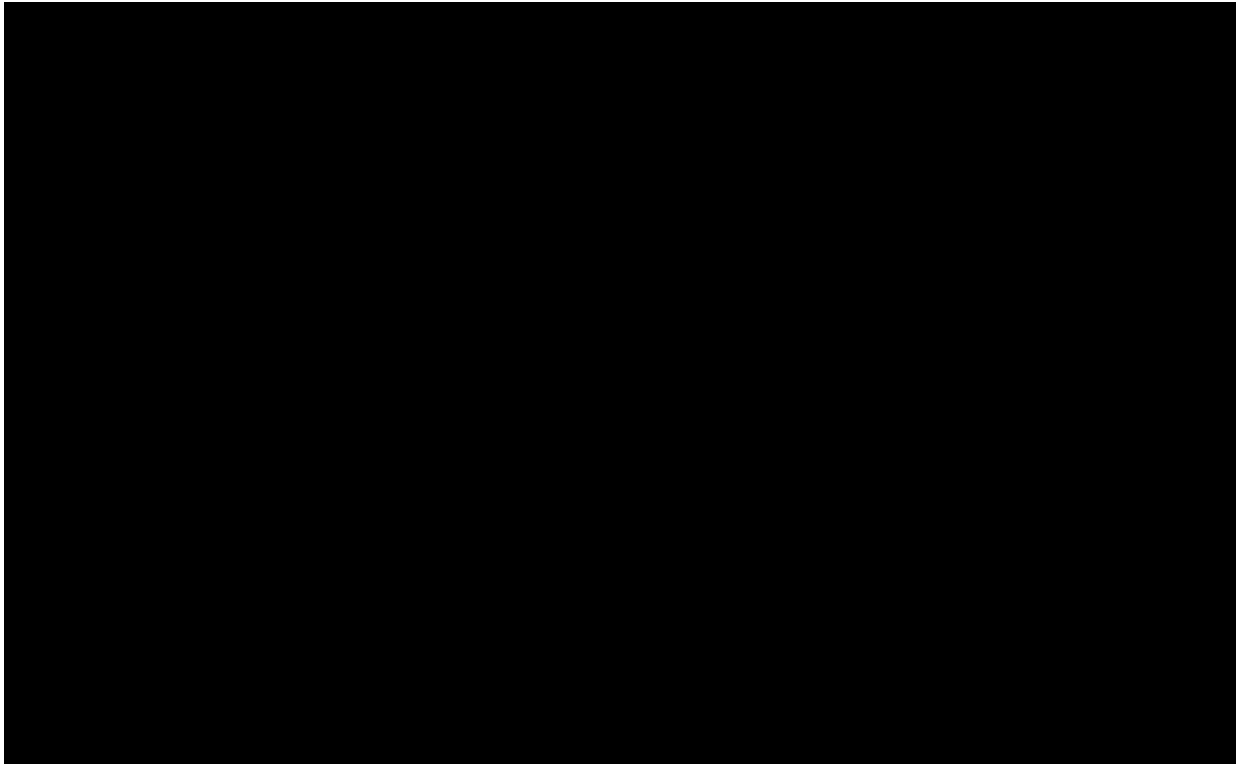
- [Redacted]
- [Redacted]
- [Redacted]

[Redacted]

[Redacted]

[Redacted]	[Redacted]
[Redacted]	[Redacted]
[Redacted]	[Redacted]
[Redacted]	[Redacted]





[Redacted text line]

- [Redacted list item 1]
- [Redacted list item 2]
- [Redacted list item 3]
- [Redacted list item 4]
- [Redacted list item 5]

[Redacted text line]

[Redacted text line]

[Redacted text line]

[REDACTED]

[REDACTED]

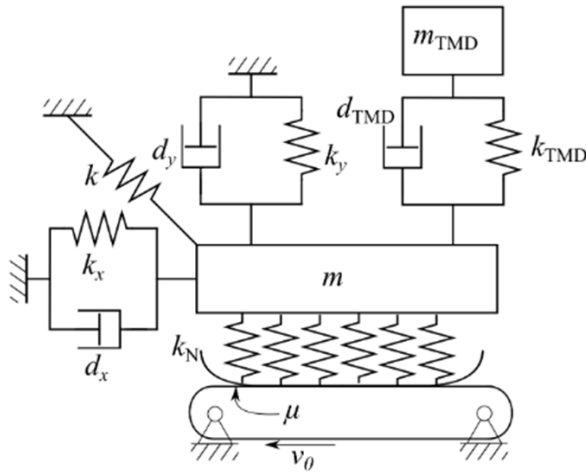
[REDACTED]

[REDACTED]

[REDACTED]

## Tuned Mass Damper (TMD)

To address the specific instability identified in measurement data ("Brake Moan"), the model was extended to include a Tuned Mass Damper (TMD). A TMD is a passive vibration absorber consisting of a secondary mass, spring, and damper attached to the primary structure. Its function is to oscillate out of phase with the primary system, transferring kinetic energy away from the unstable mode and dissipating it through its local damper, thereby reducing the real part of the system's eigenvalues into the stable region.



Schematic of the Friction Oscillator with TMD

## Model Calibration

Before designing the TMD, the baseline 2DOF model was calibrated to replicate the specific instability observed in the given measurement data. The stiffness and friction parameters were tuned via an inverse approach to match the experimentally measured eigenvalues:

- **Target Frequency:** 260 Hz (Eigenfrequency of the unstable mode).
- **Target Instability:** Growth rate of  $+12.8 \text{ s}^{-1}$  (Real part of the eigenvalue).

This calibration ensures that the subsequent TMD parameter study addresses the actual physical instability rather than a theoretical approximation.

## TMD System Setup

The TMD is attached to the vertical degree of freedom ( $y$ ) of the friction oscillator . This introduces a third degree of freedom to the system equations ( $x_{sys} = [x, y, x_{TMD}]^T$ ).

The new system matrices are constructed by expanding the calibrated base matrices ( $\mathbf{M}_{base}, \mathbf{K}_{base}, \mathbf{D}_{base}$ ). The TMD mass  $m_{TMD}$ , stiffness  $k_{TMD}$ , and damping  $d_{TMD}$  are integrated as follows:

$$\mathbf{M}_{sys} = \begin{bmatrix} \mathbf{M}_{base} & 0 \\ 0 & m_{TMD} \end{bmatrix}$$

$$\mathbf{K}_{sys} = \begin{bmatrix} K_{xx} & K_{xy} & 0 \\ K_{yx} & K_{yy} + k_{TMD} & -k_{TMD} \\ 0 & -k_{TMD} & k_{TMD} \end{bmatrix}$$

where the coupling terms ( $-k_{TMD}$ ) represent the interaction forces between the primary mass and the absorber. The damping matrix  $\mathbf{D}_{sys}$  is structured identically to the stiffness matrix.

## Parameter Study Design

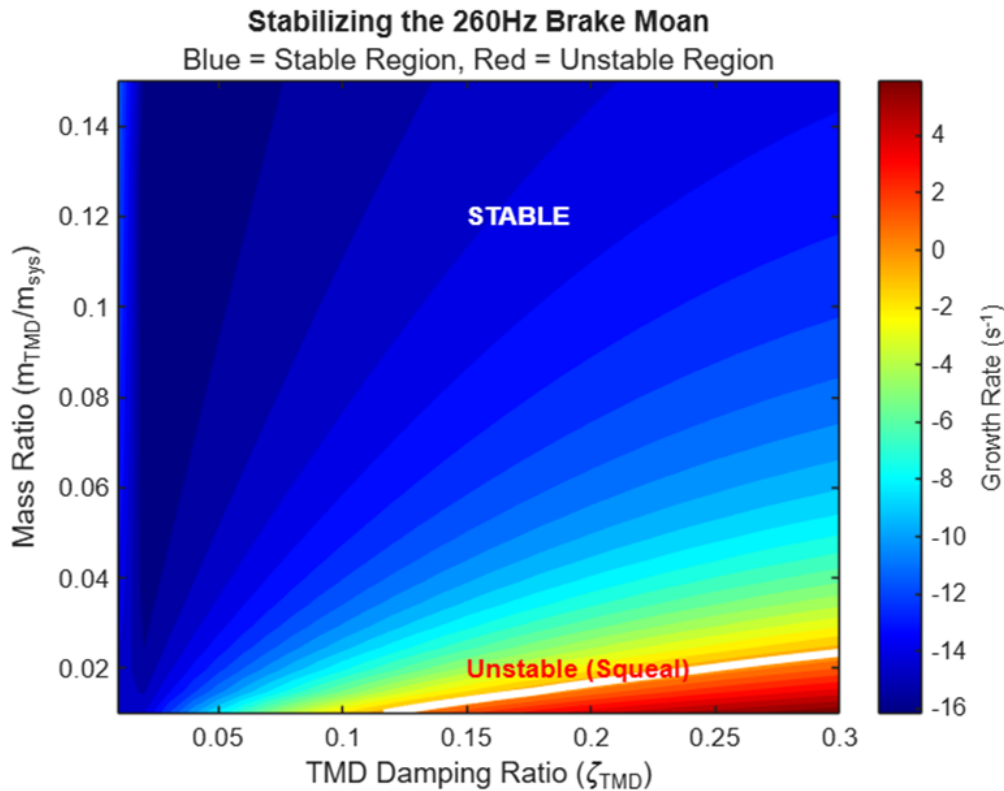
To identify the optimal design configuration, a parametric study was performed. The stability growth rate (max real part of eigenvalues) was computed for a range of TMD properties:

- **Mass Ratio** ( $\mu_{TMD} = m_{TMD}/m_{sys}$ ): Varied from 1% to 15% to evaluate the trade-off between added weight and suppression capability.
- **Damping Ratio** ( $\zeta_{TMD}$ ): Varied from 1% to 30% to find the optimal dissipation level. If  $\zeta_{TMD} = 0.1$ , it means the TMD has 10% of *its own* critical damping.

The goal is to identify the combination of parameters that shifts the system's dominant eigenvalue from the unstable region ( $\sigma > 0$ ) to the stable region ( $\sigma < 0$ ).

## TMD Parameter Study Results

The results of the parameter study are visualized in the stability map shown below:



Stability Map for the Tuned Mass Damper. white contour line marks the stability boundary ( $\sigma = 0$ )

The critical features of the plot are:

- **Unstable Region (Red/Orange):** Located at the bottom of the graph, corresponding to very low mass ratios ( $\mu_{TMD} \lesssim 2\%$  and  $\zeta_{TMD} \geq 0.12$ ). In this region, the TMD lacks sufficient inertia to counteract the friction-induced negative damping, and the system remains unstable
- **Stability Boundary (White Line):** This contour represents the "break-even" point where the effective damping provided by the TMD exactly cancels the negative damping from the friction contact.
- **Stable Region (Blue):** The majority of the design space lies in the stable region. As the mass ratio increases beyond the threshold of approximately 2.5%, the real part of the eigenvalues becomes negative, indicating that vibrations will decay over time.

The considered optimal configuration would be mass ratio of 5% ( $\mu_{TMD} = 0.05$ ) combined with a damping ratio of 10-15% ( $\zeta_{TMD} \approx 0.10 - 0.15$ ) places the system well within the deep blue "stable" zone. This provides a safety margin against parameter drift (e.g., changes in friction due to temperature or wear) while minimizing the added weight to the brake system.

One could pose the question of why a simple damper cannot be used without a secondary mass. However, if a damper was attached to the vibrating structure with its other end free (zero mass), that free end would simply move in unison with the structure. This results in zero relative velocity, generating no damping force. The TMD mass provides the essential inertia that resists motion, creating the relative velocity required for the damper to function and dissipate energy.

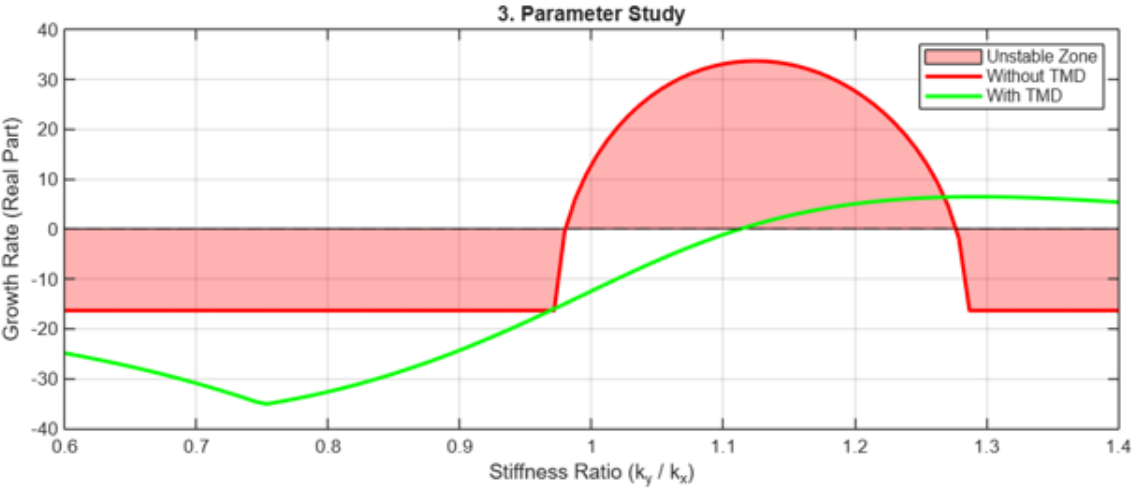
Another consideration could be that a damping ratio of 0 should also result in instability. If the damping ratio is zero ( $\zeta_{TMD} = 0$ ), the TMD can transfer kinetic energy back and forth with the primary mass (like two pendulums connected by a spring), but it has no way to dissipate that energy. Consequently, the total energy of the system would continue to accumulate due to the friction work, and the vibration amplitude would grow indefinitely (Instability). In the heatmap, the lowest damping value plotted was 1% ( $\zeta_{TMD} = 0.01$ ). If it were to be extended ( $\zeta_{TMD} = 0$ ), it would indeed be entirely red (Unstable).

### Time-Domain Verification and Robustness Study

To finalize the design, a comprehensive validation was performed to ensure the Tuned Mass Damper (TMD) is robust against parameter variations and capable of suppressing transient instability events.

In brake systems, contact stiffness is not constant; it fluctuates due to changes in pressure, temperature, and wear. A robust control measure must maintain stability even as the system parameters drift. To evaluate this, a parameter sweep was conducted, varying the vertical stiffness ratio ( $k_y/k_x$ ).

$\mu_{TMD}$	$\zeta_{TMD}$
5%	10%



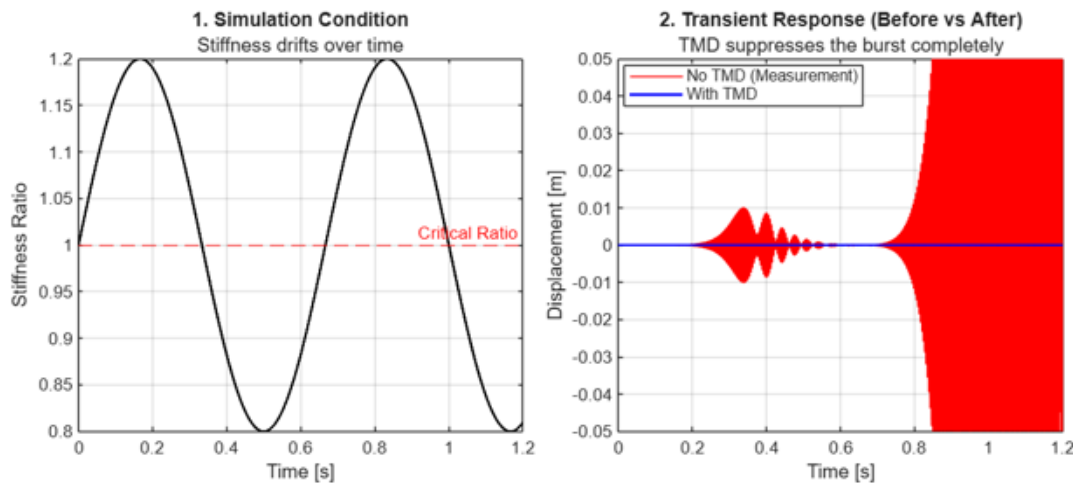
Robustness Check. The Red curve shows the baseline system’s large instability zone (Peak Growth  $\approx 35s^{-1}$ ). The Green curve shows the TMD system.

While the instability is drastically dampened, a residual unstable region remains for stiffness ratios  $> 1.1$ . This indicates that if the brake stiffness drifts significantly higher (e.g., due to thermal expansion or pressure increase), the TMD is no longer perfectly tuned to the shifting eigenfrequencies. While the "squeal" would be much quieter (lower growth rate) than the baseline, the system is technically still unstable in this off-design region.

Robustness was evaluated for 3 different cases:

- Constant Sinusoidal Oscillation
- Progressive Oscillation
- Progressive-Regressive Oscillation

## Constant sinusoidal oscillation

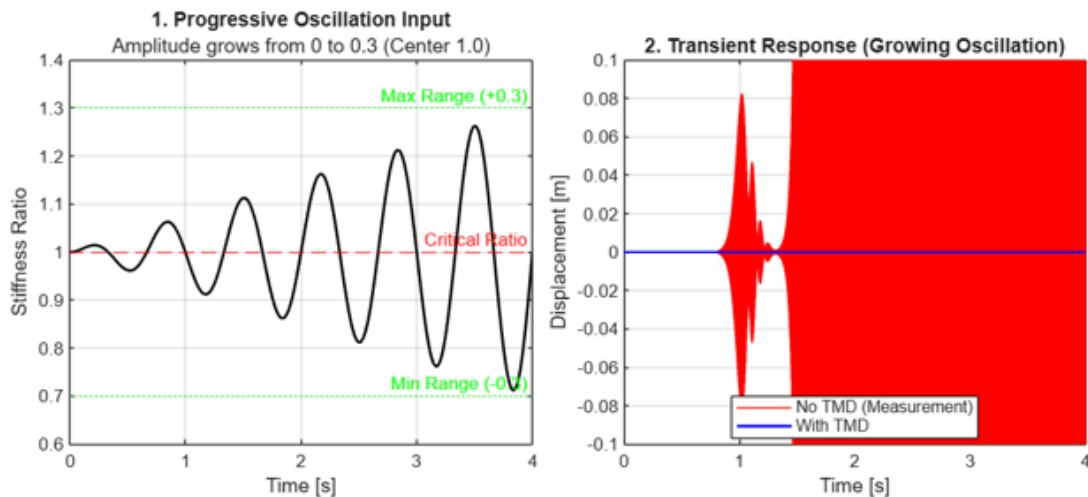


The results in the graphs above confirm the validity of the TMD design. Although the static analysis predicts instability at high stiffness ratios ( $k_y/k_x > 1.1$ ), the time-domain simulation shows no vibration growth.

This is attributed to **Dynamic Stabilization**: the residual growth rate is so low ( $\approx 2 \text{ s}^{-1}$ ) and the stiffness oscillation is sufficiently fast that the system passes through the unstable zone before vibration amplitudes can build up. The energy dissipation during the stable phases dominates the cycle, effectively suppressing the brake moan under dynamic operating conditions.

## Progressive Oscillation

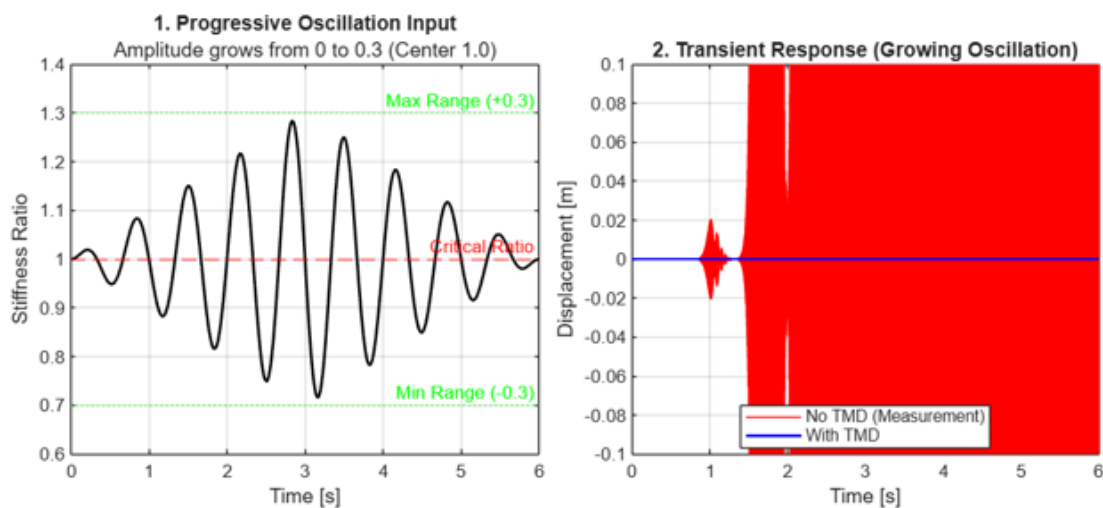
To further challenge the design, a "Progressive Oscillation" test was conducted. Instead of a fixed drift amplitude, the stiffness fluctuation was linearly increased over time (now 4s), expanding the range of ratios from [0.95, 1.05] up to [0.7, 1.3]. This simulates a scenario where operating conditions deteriorate progressively (e.g., hydraulic pressure fluctuations, temperature, etc.).



- The system without TMD (Red) tolerates small fluctuations but fails catastrophically once the drift amplitude exceeds  $\pm 10\%$  (around  $t = 1$  s), leading to immediate divergence.
- The system with TMD (Blue) withstands the entire test duration, even when the stiffness ratio swings wildly between 0.7 and 1.3. This proves that the Dynamic Stabilization effect holds even under extreme parameter variations, confirming the TMD as a definitive solution for the 260 Hz brake moan

## Progressive-Regressive Oscillation

The final robustness test simulates a complete transient event. This represents a temporary excursion into extreme operating conditions followed by a recovery:



- The system without the TMD (Red) fails as soon as the disturbance amplitude crosses the stability threshold ( $t \approx 1$  s). Even though the input disturbance eventually subsides (after  $t = 3$  s), the vibration amplitudes have already grown to catastrophic levels
- The system with the TMD (Blue) shows zero response. It successfully navigates the entire envelope of the disturbance (including the peak deviation where the stiffness ratio hits 1.3) without ever allowing the instability

to initiate. This confirms that the TMD provides a complete safeguard against temporary, severe parameter drifts.

## Non-dimensional TMD

The dimensional parameter study presented successfully identified a stable TMD configuration. However, to generalize the results and gain deeper physical insight on the model itself, a nondimensional analysis was performed. The main goal of this was to identify a small set of dimensionless groups that govern the underlying physics of the problem.

### Nondimensionalization Procedure

#### Reference Scales

The system is nondimensionalized using the following reference scales:

$$\omega_0 = \sqrt{\frac{k_y}{m}} \quad (\text{reference frequency})$$

$$\tau = \omega_0 t \quad (\text{nondimensional time})$$

This choice normalizes the vertical stiffness to unity, making the resulting parameters directly interpretable.

#### Stiffness Ratios

Parameter	Definition	Description
$K_x$	$k_x/k_y$	Tangential stiffness ratio
$K_s$	$k/k_y$	Coupling spring ratio
$K_N$	$k_N/k_y$	Contact stiffness ratio

#### Damping Parameters

$$D_i = \frac{d_i}{m\omega_0}$$

Related to the damping ratio by:

$$D_i = 2\zeta_i \sqrt{K_i}$$

## TMD Parameters

Parameter	Definition	Description
$m_R$	$m_{TMD}/m$	Mass ratio
$\gamma$	$\omega_{TMD}/\omega_0$	Frequency tuning ratio
$K_{TMD}$	$m_R\gamma^2$	Nondimensional TMD stiffness

## Nondimensional System Matrices

The dimensional matrices from the previous section transform to:

### Mass Matrix

$$\mathbf{M}^* = \begin{bmatrix} 1 & 0 & 0 \\ 0 & 1 & 0 \\ 0 & 0 & m_R \end{bmatrix}$$

### Damping Matrix

$$\mathbf{D}^* = \begin{bmatrix} D_x & 0 & 0 \\ 0 & D_y + D_{TMD} & -D_{TMD} \\ 0 & -D_{TMD} & D_{TMD} \end{bmatrix}$$

where:

$$D_{TMD} = 2\zeta_{TMD}\gamma m_R$$

### Stiffness Matrix (with coupling spring at angle $\alpha = 45^\circ$ )

$$\mathbf{K}^* = \begin{bmatrix} K_x + 0.5K_s & 0.5K_s + \mu K_N & 0 \\ -0.5K_s & 1 + 0.5K_s + K_N + m_R\gamma^2 & -m_R\gamma^2 \\ 0 & -m_R\gamma^2 & m_R\gamma^2 \end{bmatrix}$$

The asymmetry  $K_{12}^* \neq K_{21}^*$  is preserved

$$K_{12}^* - K_{21}^* = K_s + \mu K_N$$

This asymmetry is still what drives the mode-coupling instability.

## Key Dimensionless Groups

Using the Buckingham Pi theorem, two key dimensionless groups were found and could be used to characterize the instability behaviour:

Friction-Coupling Parameter ( $\Pi_1$ )

$$\Pi_1 = \mu \cdot K_N$$

This group quantifies the strength of friction-induced coupling. It appears directly in the off-diagonal asymmetry of the stiffness matrix and drives the instability. Larger values of  $\Pi_1$  increase the tendency toward unstable behavior.

Mode Frequency Ratio ( $\Pi_2$ )

$$\Pi_2 = \frac{\omega_1}{\omega_2} = \sqrt{\frac{K_x + 0.5K_s}{1 + 0.5K_s + K_N}}$$

Mode-coupling instability is strongest when  $\Pi_2 \approx 1$ , i.e., when the two modal frequencies are close.

For a general case of any coupling spring at angle  $\alpha$ , this is derived as:

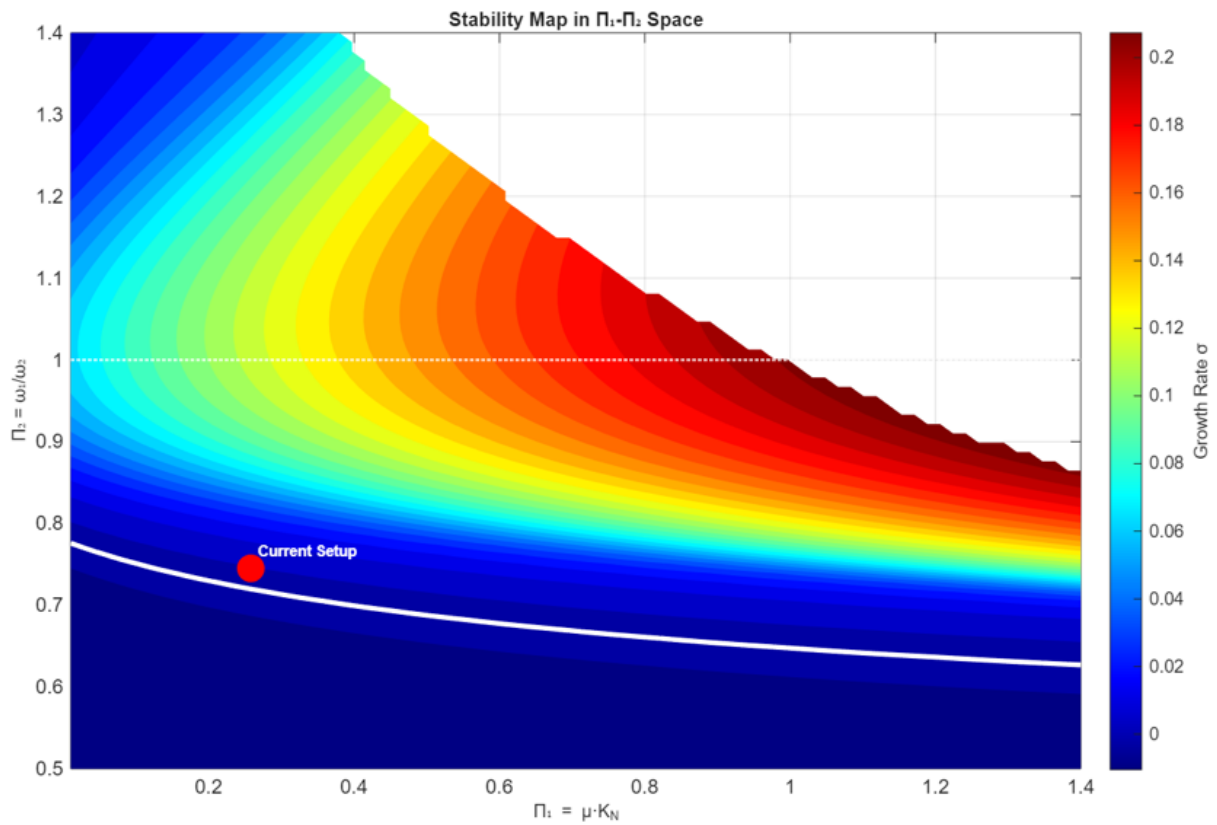
$$\Pi_2 = \frac{\omega_1}{\omega_2} = \sqrt{\frac{K_x + K_s \cos^2 \alpha}{1 + K_s \sin^2 \alpha + K_N}}$$

## Pi Groups Sweep Study and the Stability Boundary

With these adimensional groups in mind, a parameter sweep study was done in order to find more about the relationship between them and the growth rate, i.e. the instability behaviour of the TMD model. As an example case, the system setup studied with the dimensional TMD model was also pointed out.

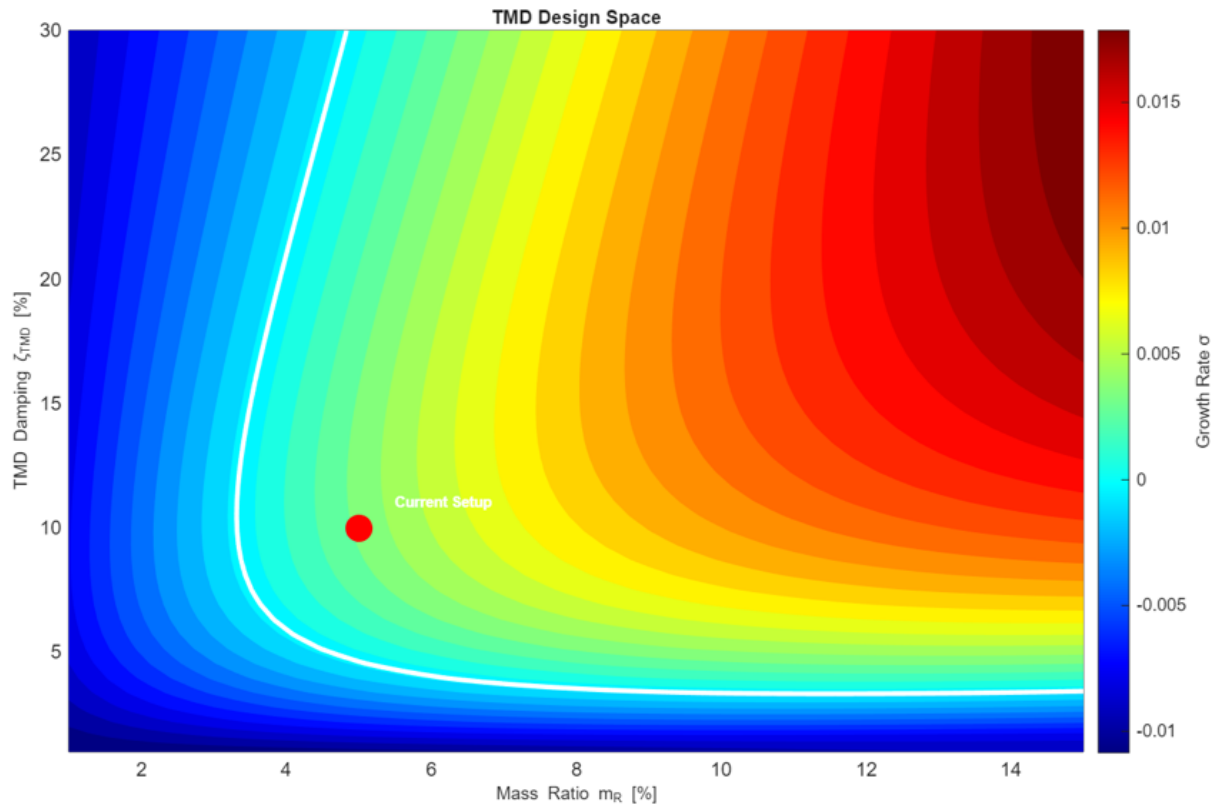
### Stability Map in $\Pi_1$ - $\Pi_2$ Space

Plotting the parameter sweep in the  $\Pi_1$ - $\Pi_2$  Space and marking the line where the growth rate was null, it was possible to observe a stability boundary that denotes stable and unstable regions in regards to the  $\Pi_1$  and  $\Pi_2$  parameters.



## Nondimensional TMD Design Space

The nondimensional TMD design space mirrors the dimensional results but expressed in terms of  $m_R$  and  $\zeta_{TMD}$  and also shows a clear stability boundary in regards to the TMD design decisions.



The optimal design region (deep blue) seems to be consistent with the dimensional analysis. The nondimensional formulation confirms that these ratios, rather than absolute values, govern TMD effectiveness.

## Conclusion

This project demonstrated the workflow for analyzing and mitigating brake moan caused by mode-coupling instability.

Some key takeaways were:

- **Mode-coupling mechanism confirmed:** The 2DOF friction oscillator model accurately captures the physics of brake moan. Instability arises when friction-induced asymmetry in the stiffness matrix causes two structural modes to coalesce, leading to positive growth rates ( $\sigma > 0$ ) beyond a critical friction coefficient.
- **Experimental validation achieved:** Real measurement data from brake calipers exhibited a clear 260 Hz instability with a positive growth rate. The model was successfully calibrated to reproduce these characteristics, bridging theoretical analysis with physical observations.
- **TMD design established:** A Tuned Mass Damper with 5% mass ratio and 10% damping ratio effectively stabilizes the system. Time-domain simulations confirmed robustness against parameter variations, including stiffness fluctuations of  $\pm 30\%$ .
- **Nondimensional framework developed:** The stability behavior is governed by two key dimensionless groups: the friction-coupling parameter  $\Pi_1$  and the mode frequency ratio

$\Pi_2$ . The resulting stability maps provide a good design tool applicable to any brake system with equivalent nondimensional parameters.

## References

1. Breuer, B., Bill, K.H. (2003). Schwingungen und Geräusche. In: Breuer, B., Bill, K.H. (eds) Bremsenhandbuch. ATZ/MTZ-Fachbuch. Vieweg+Teubner Verlag, Wiesbaden. [https://doi.org/10.1007/978-3-663-09441-8\\_22](https://doi.org/10.1007/978-3-663-09441-8_22)
2. Shin, K., Brennan, M. J., Oh, J.-E., & Harris, C. J. (2002). Analysis of disc brake noise using a two-degree-of-freedom model. *Journal of Sound and Vibration*, 254(5), 837–848. <https://doi.org/10.1006/jsvi.2001.4127>
3. Hoffmann, Norbert, Michael Fischer, Ralph Allgaier, and Lothar Gaul. 2002. "A Minimal Model for Studying Properties of the Mode-Coupling Type Instability in Friction Induced Oscillations." *Mechanics Research Communications* 29: 197–205. [https://doi.org/10.1016/S0093-6413\(02\)00254-9](https://doi.org/10.1016/S0093-6413(02)00254-9).
4. Schroth, Zum Entstehungsmechanismus des Bremsenquietschens (Fortschrittberichte VDI : Reihe 12, Verkehrstechnik, Fahrzeugtechnik Nr. 547). Düsseldorf: VDI-Verl., 2003.
5. Chatterjee, „On the Design Criteria of Dynamic Vibration Absorbers for Controlling Friction-Induced Oscillations“, *Journal of Vibration and Control*, Jg. 14, Nr. 3, S. 397-415, 2008, doi: 10.1177/1077546307080030.